Electrochemical Recognition of Aromatic Species with Ferrocenylated 1,3,5-Triazine- or 1,3,5-Triphenylbenzene-Containing Highly Organized Molecules

Aleksandra I. Kosińska[+],[a] Monika K. Nisiewicz[+],[a, b] Anna M. Nowicka,[b] and Artur Kasprzak*[a]

Two ferrocenylated organized molecules comprising 1,3,5-triphenylbenzene (**Fc-1**) or 2,4,6-triphenyl-1,3,5-triazine skeletons (**Fc-2**) were used for the first time as receptor layers for the electrochemical recognition of polycyclic aromatic hydrocarbons. While our group recently reported the synthesis of **Fc-1**, herein the facile synthesis of its 2,4,6-triphenyl-1,3,5-triazine-containing structural analog (**Fc-2**) is presented. Although the synthesis of **Fc-2** was found to be challenging, we achieved a very high yield (89%) under mild conditions using an acid-catalyzed imine-bond formation reaction in 1,4-dioxane:toluene solvent system. Title compounds were comprehensively characterized with various analytical techniques, including spectroscopic (NMR, FT-IR, FT-Raman spectroscopy) methods, high-resolution mass spectrometry (HRMS), microscopic (SEM) and electrochemical (CV) analyses. **Fc-1** and **Fc-2** were also used for the construction of the first-of-a-kind recognition layers (electrochemical sensors) dedicated to the recognition of polycyclic aromatic hydrocarbons. Fully constructed innovative sensors enabled the efficient recognition of analytes since the limit of detection (LOD) values were not higher than 2.9 μM. Comparative studies between the working parameters of electrochemical sensors comprising **Fc-1** or **Fc-2** were also included in this work.

Introduction

Self-assembly and dynamic covalent chemistry concepts have emerged as useful tools toward the selective and efficient formation of highly organized molecules in a specific manner.[1–3] The importance of as-fabricated compounds results not only from their interesting properties and structures, but also from the number of potential applications in many important fields, such as catalysis[4–6] or medicine.[7–9] Cage or cage-like compounds, which are commonly synthesized by utilizing dynamic covalent chemistry concepts starting from various building blocks, act as the prominent class of highly organized organic compounds for various applications.[10–15]

Importantly, the introduction of redox-active species to the above-discussed molecules is an interesting approach toward tuning their properties and functions and opening new areas of applications.[16–19] Ferrocene (Fc), a redox-active metallocene, is commonly a first- or best-choice molecule for such purpose, because of its stability in air, good solubility in many organic solvents, as well as its electrochemical and thermal stability.[20,21] Additionally, its redox process (the presence of ferrocene/ferrocenium cation (Fc/Fc^+) redox couple) is single-electron, reversible and is characterized by the high electron transfer rate. Because of these beneficial features, Fc is commonly employed motif for the construction of the sensor layers dedicated to the recognition of various analytes.[20–23] In the last several years, interesting works dealing with the preparation of Fc containing molecular cages were published.[24–34] From the viewpoint of the construction of these highly organized molecules, Fc offers interesting perspectives related to a dynamic flexibility of the cyclopentadienyl rings (*anti* or *syn* rotation phenomenon). Most commonly, organized molecules composed of 1,1′-disubstituted ferrocenes adopting the *syn* conformation were reported.[28–34] However, some specific Fc based ligands, such as rotationally flexible ones,[24,25,33,34] offered the possibility to construct either cage structures in which 1,1′-disubstituted ferrocenes adopted the *anti* conformation[24,25] or intriguing low-symmetry architectures in which 1,1′-disubstituted Fc's cyclopentadienyl rings were twisted.[26] Additionally, cage products that feature a confined cavity motif were shown to incorporate some specific guest molecules, such as *p*-toluenesulfonate anion.[24,32] Importantly, chemical oxidation assays[26] (formation of Fc^+) revealed that redox activity is assured in such specific cage products; However, preliminary electrochemical trials suggested that host-guest inclusion process might not cause the drastic changes in redox potentials of the cage.[24,32] Nevertheless, it should be highlighted that these innovative studies were published very recently (2019–2021) and without any doubt the chemistry of ferrocenylated highly organized organic molecules offers many more perspectives and functions.

In 2020 we reported the synthesis of a C_3-symmetric ferrocenylated 1,3,5-triphenylbenzene containing highly ordered molecule (**Fc-1**; Figure 1).[35] To our delight, we found that imine-bond containing **Fc-1** can be selectively and effectively

[a] *A. I. Kosińska,[+] M. K. Nisiewicz,[+] Dr. A. Kasprzak*
Faculty of Chemistry
Warsaw University of Technology
Noakowskiego Str. 3, 00-664 Warsaw (Poland)
E-mail: akasprzak@ch.pw.edu.pl
[b] *M. K. Nisiewicz,[+] Prof. A. M. Nowicka*
Faculty of Chemistry
University of Warsaw
Pasteura Str. 1, 02-093 Warsaw (Poland)
[+] *These authors contributed equally to this work.*
Supporting information for this article is available on the WWW under https://doi.org/10.1002/cplu.202100137

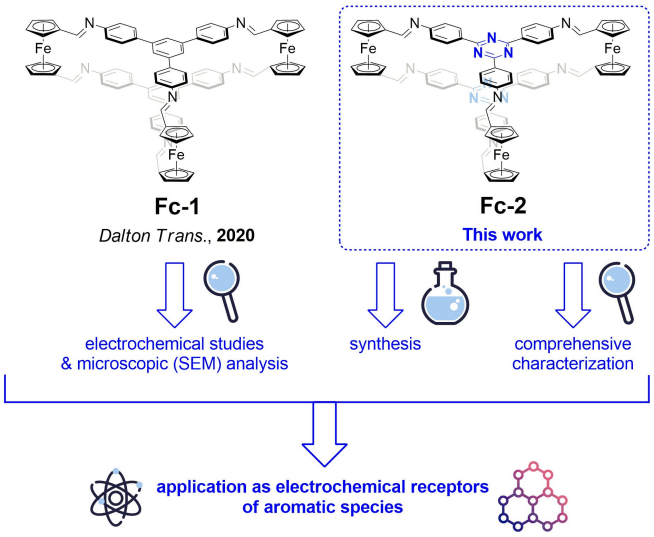

Figure 1. Graphical representation of the contents and aims of this work.

formed starting from 1,3,5-(4-aminophenyl)benzene and 1,1′-diformylferrocene for which *syn* conformation of cyclopentadienyl rings with π-stacked aromatic substituents was favored in the reaction course. **Fc-1** can be obtained in excellent 95% isolated yield without any traces of oligomeric products and low or high molecular weight species. Importantly, we also unraveled **Fc-1**'s ability to non-covalently interact with aromatic compounds by means of a dynamic π-π stacking-like non-covalent forces (^{1}H NMR, ^{1}H DOSY NMR, cold-spray ESI-MS and emission spectra experiments). Inspired by this work, herein, we report the method for the preparation of respective Fc-tethered highly organized molecule that comprises 1,3,5-triazine skeletons (**Fc-2**; for the graphical representation of the contents and aims of this work, see Figure 1). While the chemistry of 2,4,6-(4-aminophenyl)-1,3,5-triazine derived imines offers many encouraging perspectives and applications,[36–38] the synthesis can be challenging, mainly because of limited reactivity and solubility of these compounds in comparison to their hydrocarbon derivatives. Furthermore, in pursuit of novel applications of ferrocenylated highly organized molecules we investigated fully innovative application of **Fc-1** and **Fc-2** as the first electrochemical receptors of polycyclic aromatic hydrocarbons.

Results and Discussion

Fc-1 was obtained following the literature procedure.[35] 2,4,6-Tris(4-aminophenyl)-1,3,5-triazine (**2**) was obtained by means of the acid-catalyzed trimerization reaction starting from 4-aminobenzonitrile.[36] Having **2** at hand, we have initiated the synthetic studies toward the preparation of **Fc-2** using 1,1′-diformylferrocene (**1**; Fc-$(CHO)_2$) as the starting material (Scheme 1). It is worth to stress that **Fc-1**, which from the structural viewpoint is the origin molecule of **Fc-2**, can be easily and efficiently synthesized[35] at room temperature using **1** and 1,3,5-tris(4-aminophenyl)benzene as the starting materials and ethanol[39] as the solvent. However, our screening experiments revealed that the usage of ethanol as the solvent for **Fc-2** synthesis did not provide the desired product (starting material **2** has been recovered, only). We hypothesize that this could be a result of significantly lower solubility in ethanol of 1,3,5-triazine-containing **2** in comparison to the respective 1,3,5-tris(4-aminophenyl)benzene. This feature might cause instability and/or insolubility of the intermediate products what prevents the formation of **Fc-2**. Therefore, our efforts focused on changing the solvent and reaction conditions. At first, we tested the reaction conditions (*o*-dichlorobenzene : *n*-butanol solvent system) recently reported for the covalent-organic framework (COF) material.[40] While this approach provided satisfactory results (reaction yield in the respect to **Fc-2** was equal to *ca.* 40%), this methodology employed harsh reaction conditions (reaction temperature 100 °C) together with long reaction times (72 hours) what also lead to the formation of some oligomeric-like side products. In the search of more beneficial process conditions, the acid-catalyzed reaction in 1,4-dioxane with the addition of other solvent (methanol, toluene, *o*-dichlorobenzene or chlorobenzene) was explored. These experiments were performed at room temperature. It was found that these reaction conditions provided excellent yields of the target product **Fc-2**. The highest reaction yield (89%) was found in 1,4-dioxane:toluene (1:3 *v*/*v*) solvent system using acetic acid as the catalyst (reaction time 48 hours; see experimental section for the details). The designed protocol was also easy-to-perform, as **Fc-2** was isolated from the reaction mixture by simple filtration and was purified by washing with solvents (see experimental section). Based on these synthetic studies, we claim that 1,4-dioxane provided good solubility of both starting materials and mono- or double-ferrocenylated imines; Thus, this

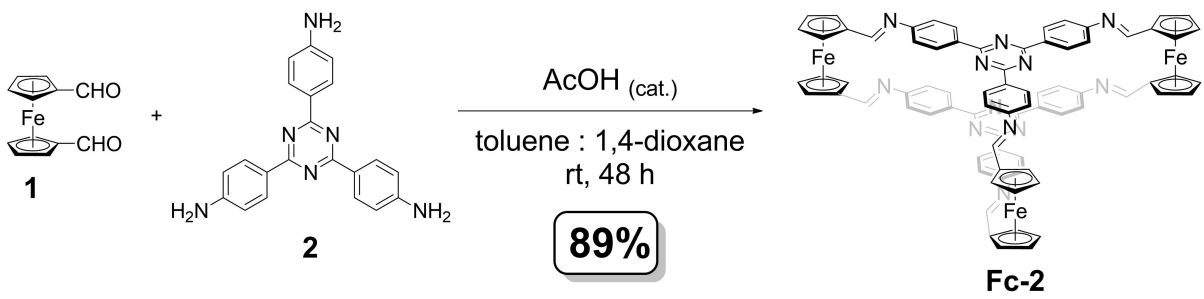

Scheme 1. Synthesis of **Fc-2**.

solvent enabled the very efficient formation of the target product **Fc-2**.

The ^{1}H NMR spectrum measured in THF-d_8[41] revealed that the target C_3-symmetric **Fc-2** was successfully synthesized, since 5 groups of signals, including (*i*) triplet-like multiplets characteristic for 1,1′-disubstituted ferrocenes, (*ii*) the peaks originating from the presence of 2,4,6-triphenyl-1,3,5-triazine skeleton and (*iii*) the peak originating from the presence of the imine-type linkage, were observed (9.0–3.8 ppm inset of the ^{1}H NMR spectrum[42] is presented in Figure 2a). While sufficient ^{13}C NMR data could not be collected because of highly limited solubility of **Fc-2**, ^{1}H DOSY NMR experiment confirmed that the sample was composed of one type of molecule (**Fc-2**), only (8.9–4.0 ppm inset of ^{1}H DOSY NMR spectrum[42] is presented in Figure 2b).

Fc-2 was also subjected to Fourier-transform infrared spectroscopy (FT-IR). FT-IR spectrum of **Fc-2** (Figure 3a) featured several strong or medium intensity absorption bands that were ascribed to the C=N vibrations coming from the imine-type and 1,3,5-triazine moieties[43] (*e.g.*, 1577, 1416, 1252 cm^{-1}) and the vibrations characteristic for the 1,1′-disubstituted ferrocenes[44] (*e.g.*, 1497, 1357, 1142, 807 cm^{-1}). These observations suggesting the formation of **Fc-2** were further supported by the FT-Raman spectra analysis (Figure S3, Supporting Information). High-resolution mass spectrometry (HRMS; Figure 3b; survey ESI-HRMS spectrum was also measured, see Figure S4, Supporting Information) together with elemental analysis (see the experimental section for the details) ultimately confirmed that pure **Fc-2** was synthesized. Scanning electron microscopy (SEM; Figure 3c) studies revealed that **Fc-2** formed petal-like quasi-homogeneous objects, similarly to **Fc-1** (for data, see Section S4, Supporting Information). Additionally, energy-dispersive X-ray spectroscopy (EDS; for the EDS profile, see Figure S5, Supporting Information) confirmed that the **Fc-2** sample is composed of nitrogen, carbon, and iron (the estimated at% values for these elements were highly consistent with the calculated data).

The presence of Fc units makes the studied compounds **Fc-1** and **Fc-2** electroactive. Because only **Fc-1** compound was characterized by well solubility in dichloromethane (DCM), the

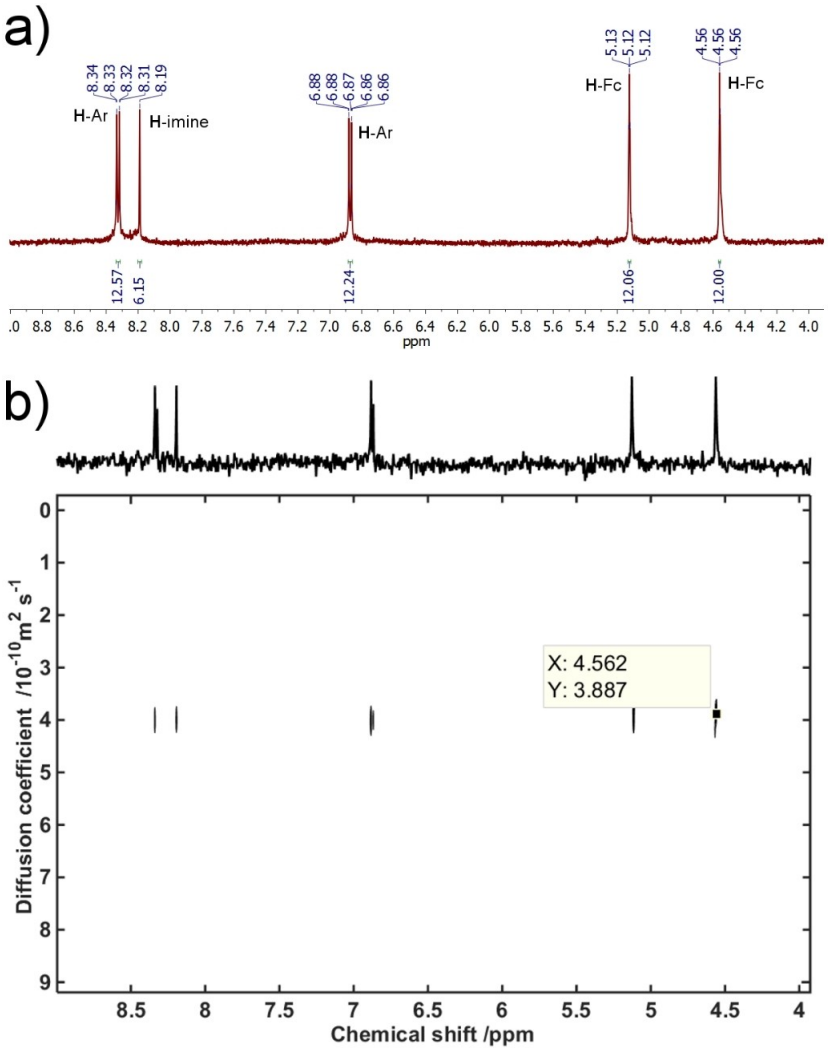

Figure 2. (**a**) 9.0–3.8 ppm inset of ^{1}H NMR spectrum (THF-d_8, 500 MHz) of **Fc-2**; (**b**) 8.9–4.0 ppm inset of ^{1}H DOSY NMR spectrum (THF-d_8, 500 MHz) of **Fc-2**. The peaks assignments are also presented in (**a**).

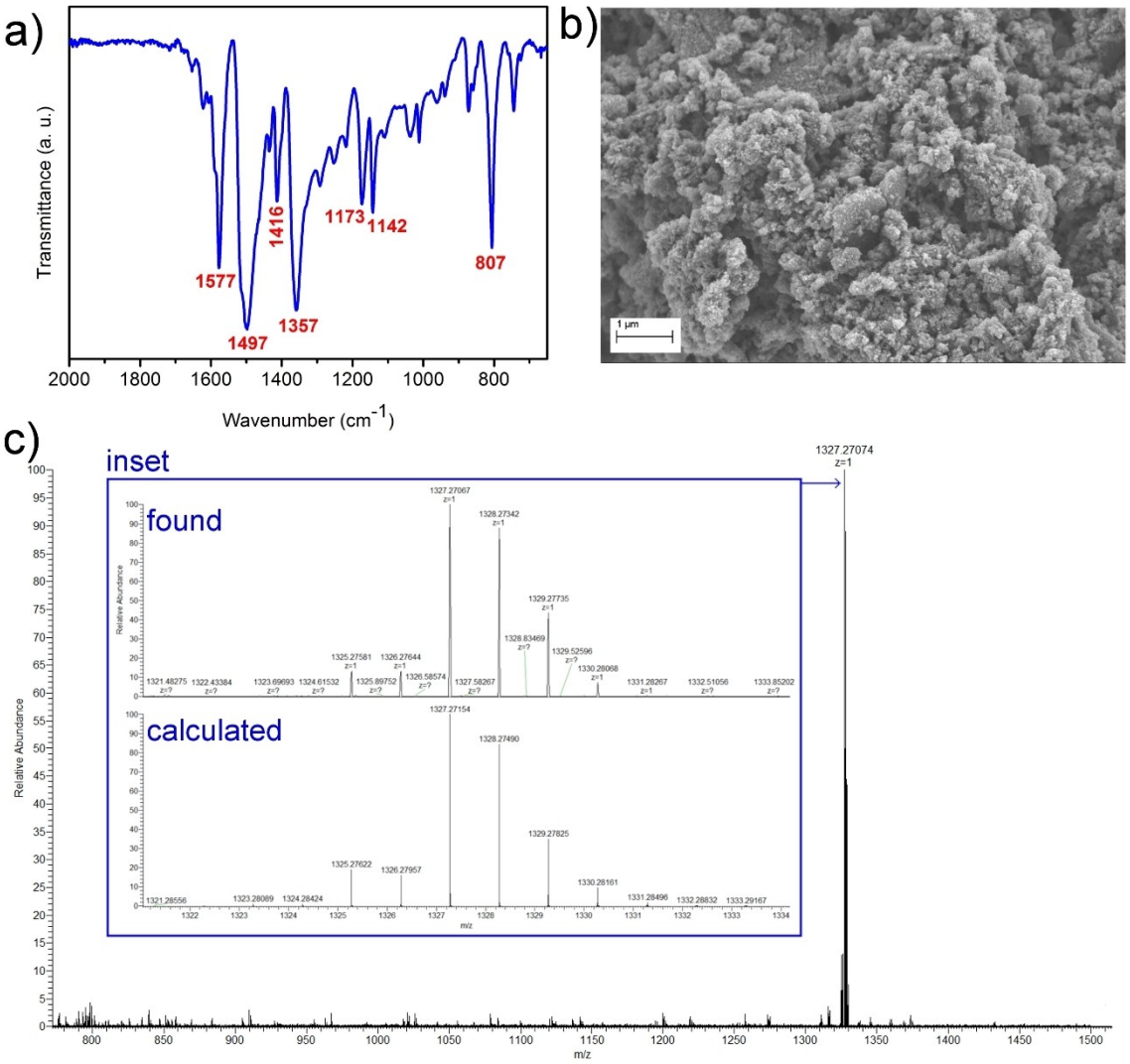

Figure 3. (**a**) FT-IR spectrum, (**b**) representative SEM image, (**c**) ESI-HRMS (TOF) spectrum (the inset is also presented) of **Fc-2**.

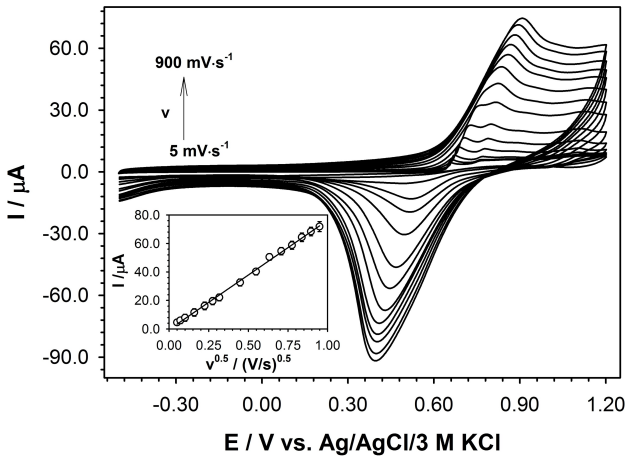

Figure 4. Cyclic voltammograms of **Fc-1** recorded in dichloromethane. Experimental conditions: $c_{Fc\text{-}1} = 1$ mM, $c_{Bu4NPF6} = 0.1$ M, $T = 21$ °C. Inset: dependence of anodic peak current vs. square root of scan rate.

electrochemical characteristic for this compound was performed in the solution. To get the information about the mechanism of oxidation and reduction process of this compound, the cyclic voltammograms (CVs) were recorded at different scan rate range from 0.005 to 0.9 $V \cdot s^{-1}$. The cyclic voltammograms of the **Fc-1** compound exhibited well-defined oxidation and reduction peaks corresponding to the $Fe^{2+/3+}$ redox couple in the Fc molecule in over the entire scan rate range. The representative CV curves for all tested scan rate are presented in Figure 4. Current depends linearly on the square root of the scan rate, which means the process is diffusion controlled. The diffusion coefficient of **Fc-1** derivative was calculated from the slope of the plot of anodic peak current versus square root of the scan rate, according to the Randles-Sevcik equation,[45] and equals to $0.604 \cdot 10^{-6}$ $cm^2 \cdot s$.

It is noteworthy that our previous studies (^{1}H NMR, ^{1}H DOSY NMR, cold-spray ESI-MS and emission spectra experiments) revealed that **Fc-1** can interact with aromatic species by means of dynamic π-π stacking-like non-covalent forces.[35] This

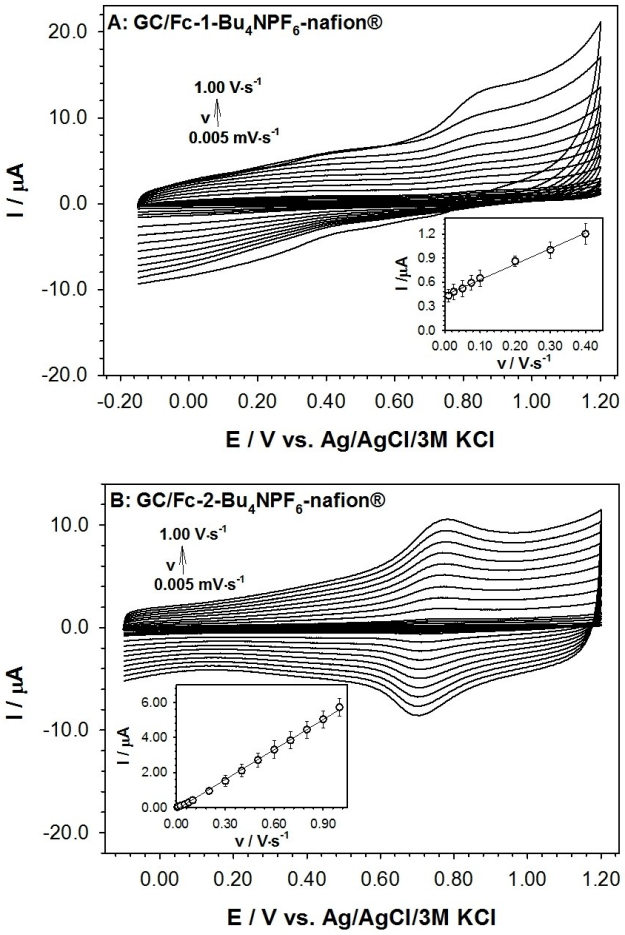

Figure 5. Cyclic voltammograms of the recognition layer, obtained from **Fc-1** (A) and **Fc-2** (B) on GC electrode in 0.1 M Bu_4NPF_6 solution in DCM for scan rates in range 0.005–1.0 $V{\cdot}s^{-1}$. Insets: plots of anodic peak currents vs. scan rate.

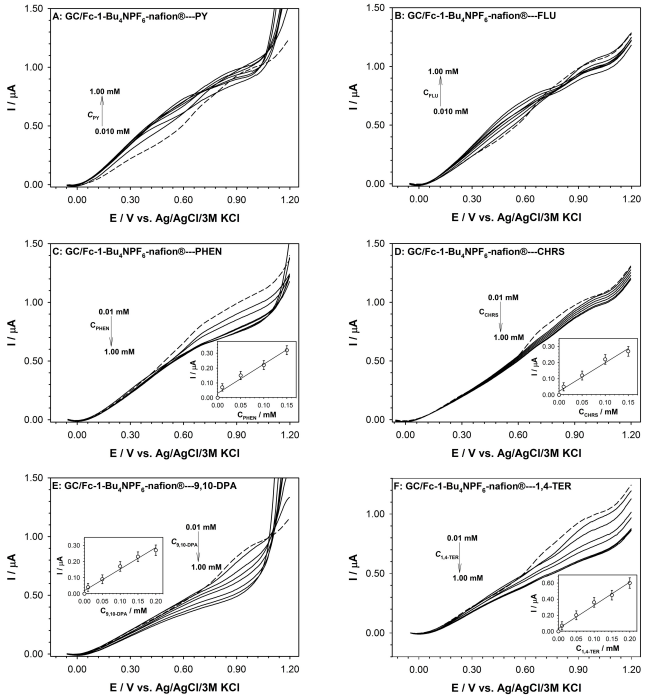

Figure 6. DPV voltammograms of the GC/**Fc-1**-Bu_4NPF_6-Nafion® receptor in 0.1 M Bu_4NPF_6 solution in DCM for various aromatic compounds concentrations in solution. Insets: plots of anodic peak currents vs. analyte concentration.

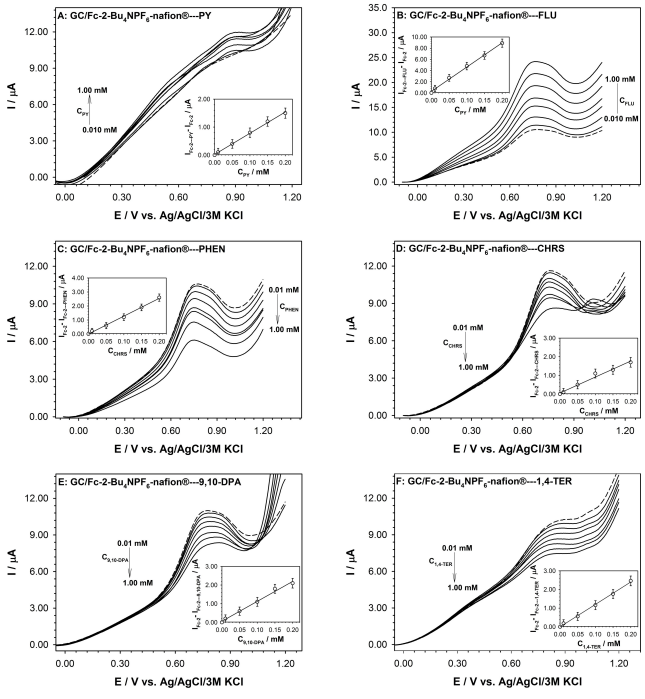

Figure 7. DPV voltammograms of the GC/**Fc-2**-Bu_4NPF_6-Nafion® receptor in 0.1 M Bu_4NPF_6 solution in DCM for various aromatic compounds concentrations in solution. Insets: plots of anodic peak currents vs. analyte concentration.

observation was further supported by our works on 1,3,5-triphenylbenzene containing dendritic molecule.[46] Furthermore, our studies on the interactions between **Fc-2** and pyrene as the representative aromatic molecule revealed that this interaction can be characterized by the similar apparent association constant (K_{app}) value as for the pyrene-**Fc-1** system reported previously;[35] The estimated K_{app} value for pyrene-**Fc-2** system equals to $5.1(2)\cdot10^2\ M^{-1}$ (Gibbs free energy (ΔG) value is $-15.5\ kJ\cdot mol^{-1}$; see data and calculation details in Section S6, Supporting Information). For comparison, for the pyrene-**Fc-1** system, K_{app} and ΔG equal to $4.0(3)\cdot10^2\ M^{-1}$ and $-14.9\ kJ\cdot mol^{-1}$, respectively.[35] Additionally, ^1H NMR titration experiment for the pyrene-**Fc-2** system (see data in Section S7, Supporting Information) revealed the same interaction type as for the pyrene-**Fc-2** system;[35] The existence of shielding effects for the **Fc-2**'s ^1H NMR spectra measured in the presence of the molar excess of pyrene further suggested that these molecules might indeed interact with each other by means of non-covalent forces. Therefore, taking into account above findings and literature premises, herein we decided to engineer a fully innovative application of ferrocene-containing **Fc-2** and **Fc-1** as the electrochemical receptors of aromatic species. It is worth to stress that the recognition of aromatic molecules, including polycyclic aromatic hydrocarbons, is of the highest environ-

mental importance because of their documented toxicity. The synthesized compounds **Fc-1** and **Fc-2** were therefore applied as receptors of aromatic compounds. For this purpose, the compounds **Fc-1** or **Fc-2** were deposited on the electrode surface. The CVs of the recognition layers (GC/Fc-Bu_4NPF_6-Nafion®), obtained at the scan rates ranging from 0.005 to 1.0 $V \cdot s^{-1}$, exhibited well-defined oxidation and reduction peaks corresponding to the $Fe^{2+/3+}$ redox couple in the ferrocene unit. They are presented in Figure 5. The CV redox peak currents scale linearly with the potential scan rate (insets in Figures 5A and 5B), and this indicates the surface confined electrochemical response, as it is expected for such films.

The sensitivity of **Fc1** and **Fc-2**-receptors versus selected aromatic compound, namely: pyrene (PY), chrysene (CHRS), fluorene (FLU), phenanthrene (PHEN), 9,10-diphenylanthracene (9,10-DPA) and 1,4-terphenyl (1,4-TER), was characterized analytically *via* the Fc oxidation current signal: functions of the differential pulse voltammograms (DPV) *versus* concentration of the selected aromatic compound (Figures 6 and 7). Regardless of the type of aromatic compounds, along with the increase in analyte concentration in the analyzed solution, significantly more intense quenching of current signals was observed in the case of **Fc-1** receptor. Specific behavior was observed in the case of **Fc-2** receptor; the Fc current signal was significantly enhanced in the presence of pyrene and fluorene. In the case of other aromatic compounds, the signal gradually decreased as the concentration of the analyte in the solution increased. Taking into account the structure of the Fc receptors it can be assumed that the studied aromatic compounds interact with these Fc-receptors through a dynamic π-π stacking process. This dynamic non-covalent process occurs when ligands (analytes) of an appropriate size and chemical nature fit themselves in with the phenyl rings. These ligands are mostly polycyclic, aromatic, and planar. The pyrene and fluorene have smaller planar fragment to form the non-covalent system with Fc-receptor, thus, they rather play a role of a bridge between Fc residues facilitating the exchange of an electron. The difference in the intensities of the current signals of the Fc units in the recognition layers before and after binding an analyte as a function of its concentration were applied to construction of the calibration curves, see insets in Figure 6 and 7. Based on these plots, analytical parameters such as linear regression equations, detection limits and relative standard deviations (RSD) were determined and are given in Table 1. In the concentration range of aromatic compounds from 10 to 150 or 200 μM the dependencies between the current signal and the concentration are linear. However, the calibration plots obtained for GC/**Fc-2**-Bu_4NPF_6-Nafion® receptor have much better sensitivity as compared to GC/**Fc-1**-Bu_4NPF_6-Nafion® receptor. For all examined concentrations of aromatic compounds from the analytical range the repeatability was good, and the relative standard deviation was less than 5% ($n = 3$). The electrode-to-electrode reproducibility was also tested with nine different electrodes, and the relative standard deviation was lower than 6%. The value of LOD was calculated as the mean background value plus 3 standard deviations($\overline{x} \pm 3\sigma$; $n = 3$). The created receptor layers enabled effective recognition of the studied aromatic species, with the LOD values equaling to 0.5–2.9 μM.

Conclusion

In conclusion, we demonstrated that the ferrocenylated 2,4,6-triphenyl-1,3,5-triazine-containing highly organized ferrocenylated molecule **Fc-2**, and a structural analog 1,3,5-triphenylbenzene containing compound **Fc-1**, can be efficiently obtained under mild conditions (isolated yield of 89% at room temperature). Optimization experiments revealed that 1,4-dioxane was the key solvent, enabling the efficient formation of the target compound. The formation of the target C_3-symemtric **Fc-2** was confirmed with various analytical techniques, including spectroscopic (NMR, FT-IR, FT-Raman) and microscopic (SEM) ones. Electrochemical analyses revealed one pair of oxidation-reduction potentials for the studied Fc-doped compounds. **Fc-1** and **Fc-2** were applied to the construction of the fully innovative recognition layers (electrochemical sensors) toward the recognition of selected polycyclic aromatic species, namely pyrene, chrysene, fluorene, phenanthrene, 9,10-diphenylanthracene and 1,4-terphenyl. The calculated LOD values were low (0.5–2.9 μM), which means that the **Fc-1** or **Fc-2** receptors provide good parameters of the constructed sensors. Our work expands the state-of-the-art of nitrogen-doped highly ordered molecules bearing a ferrocene motif and their applications as functional materials. Our future works in this topic will include the preparation of **Fc-2**- and **Fc-1**-related structures, as well as the examination of their new properties and functions.

Table 1. Analytical parameters of GC/Fc-Bu_4NPF_6-Nafion® receptors.

Linear regression equation	R^2	Analytical range [μM]	LOD [μM]	RSD [%]
		GC/Fc-1-Bu_4NPF_6-Nafion®		
$\Delta I = (2.0 \pm 0.2)C_{PHEN} + (0.03 \pm 0.02)$	0.985	10–150	2.9	3.7
$\Delta I = (1.8 \pm 0.2)C_{CHRS} + (0.02 \pm 0.01)$	0.986	10–150	2.6	3.4
$\Delta I = (1.3 \pm 0.1)C_{9,10\text{-}DPA} + (0.02 \pm 0.01)$	0.991	10–200	2.4	4.9
$\Delta I = (2.9 \pm 0.2)C_{1,4\text{-}TER} + (0.04 \pm 0.01)$	0.994	10–200	1.5	4.5
		GC/Fc-2-Bu_4NPF_6-Nafion®		
$\Delta I = (7.6 \pm 0.2)C_{PYR} + (0.02 \pm 0.02)$	0.999	10–200	1.2	3.6
$\Delta I = (43.3 \pm 1.2)C_{FLU} + (0.3 \pm 0.13)$	0.998	10–200	0.5	3.5
$\Delta I = (12.7 \pm 0.4)C_{PHEN} + (0.01 \pm 0.01)$	0.998	10–200	1.1	2.7
$\Delta I = (8.5 \pm 0.6)C_{CHRS} + (0.06 \pm 0.07)$	0.995	10–200	1.0	2.8
$\Delta I = (10.7 \pm 0.6)C_{9,10\text{-}DPA} + (0.06 \pm 0.06)$	0.995	10–200	1.4	3.4
$\Delta I = (12.0 \pm 0.3)C_{1,4\text{-}TER} + (0.01 \pm 0.03)$	0.999	10–200	0.9	3.2

Acknowledgements

Financial support from Warsaw University of Technology (WUT) is gratefully acknowledged. This work implemented as a part of Operational Project Knowledge Education Development 2014–2020 co-financed by European Social Fund, Project No POWR.03.02.00-00-I007/16-00 (POWER 2014–2020).

Conflict of Interest

The authors declare no conflict of interest.

Keywords: amines · electrochemistry · hydrocarbons · metallocenes · sensors

[1] Y. Jin, C. Yu, R. J. Denman, W. Zhang, *Chem. Soc. Rev.* **2013**, *42*, 6634–6654.
[2] S. J. Rowan, S. J. Cantrill, G. R. L. Cousins, J. K. M. Sanders, J. F. Stoddart, *Angew. Chem. Int. Ed.* **2002**, *41*, 898–952; *Angew. Chem.* **2002**, *114*, 938–993.
[3] J. Hu, S. K. Gupta, J. Ozdemir, M. H. Beyzavi, *ACS Appl. Nano Mater.* **2020**, *3*, 6239–6269.
[4] M. Yoshizawa, M. Tamura, M. Fujita, *Science* **2006**, *312*, 251–254.
[5] T. Murase, Y. Nishijima, M. Fujita, *J. Am. Chem. Soc.* **2012**, *134*, 162–164.
[6] C. J. Brown, F. D. Toste, R. G. Bergman, K. N. Raymond, *Chem. Rev.* **2015**, *115*, 3012–3035.
[7] H. Sepehrpour, W. Fu, Y. Sun, P. J. Stang, *J. Am. Chem. Soc.* **2019**, *141*, 14005–14020.
[8] S. Bhattacharyya, M. Venkateswarulu, J. Sahoo, E. Zangrando, M. De, P. S. Mukherjee, *Inorg. Chem.* **2020**, *59*, 12690–12699.
[9] G.-Y. Wu, X. Shi, H. Phan, H. Qu, Y.-X. Hu, G.-Q. Yin, X.-L. Zhao, X. Li, L. Xu, Q. Yu, H.-B. Yang, *Nat. Commun.* **2020**, *11*, article no. 3178.
[10] N. Ahmad, H. A. Younus, A. H. Chughtai, F. Verpoort, *Chem. Soc. Rev.* **2015**, *44*, 9–25.
[11] F. Beuerle, B. Gole, *Angew. Chem. Int. Ed.* **2018**, *57*, 4850–4878; *Angew. Chem.* **2018**, *130*, 4942–4972.
[12] E. G. Percástegui, T. K. Ronson, J. R. Nitschke, *Chem. Rev.* **2020**, *120*, 13480–13544.
[13] T. Hasell, A. I. Cooper, *Nat. Rev. Mater.* **2016**, *1*, article no. 16053.
[14] T. Kunde, E. Nieland, H. V. Schröder, C. A. Schalley, B. M. Schmidt, *Chem. Commun.* **2020**, *56*, 4761–4764.
[15] Q. Zhu, X. Wang, R. Clowes, P. Cui, L. Chen, M. A. Little, A. I. Cooper, *J. Am. Chem. Soc.* **2020**, *142*, 16842–16848.
[16] V. Croue, S. Goeb, M. Salle, *Chem. Commun.* **2015**, *51*, 7275–7289.
[17] S. R. Scottwell, J. D. Crowley, *Chem. Commun.* **2016**, *52*, 2451–2464.
[18] L.-X. Cai, S.-C. Li, D.-N. Yan, L. P. Zhou, P. Guo, F. Sun, *J. Am. Chem. Soc.* **2018**, *140*, 4869–4876.
[19] G. Szalóki, S. Krykun, V. Croué, M. Allain, Y. Morille, F. Aubriet, V. Carré, Z. Voitenko, S. Goeb, M. Sallé, *Chem. Eur. J.* **2018**, *24*, 11273–11277.
[20] K. Heinze, H. Lang, *Organometallics* **2013**, *32*, 5623–5625.
[21] D. Astruc, *Eur. J. Inorg. Chem.* **2017**, 6–29.
[22] M. Saleem, H. Yu, L. Wang, Zain-ul-Abdin, H. Khalid, M. Akram, N. M. Abbasi, J. Huang, *Anal. Chim. Acta.* **2015**, *876*, 9–25.
[23] H. Beitollahi, M. A. Khalilzadeh, S. Tajik, M. Safaei, K. Zhang, H. W. Jang, M. Shokouhimehr, *ACS Omega* **2020**, *5*, 2049–2059.
[24] R. A. S. Vasdev, J. A. Findlay, A. L. Garden, J. D. Crowley, *Chem. Commun.* **2019**, *55*, 7506–7509.
[25] The conformation change from *syn* to *anti* can be also changed by the metal complexation process, see: S. R. Scottwell, J. E. Barnsley, C. J. McAdam, K. G. Gordon, J. D. Crowley, *Chem. Commun.* **2017**, *53*, 7628–7631.
[26] A. J. Plajer, F. J. Rizzuto, L. K. S. von Krbek, Y. Gisbert, V. Martinez-Agramunt, J. R. Nitschke, *Chem. Sci.* **2020**, *11*, 10399–10404.
[27] N. Jiang, Z. Yuan, T. Li, Y. Zhu, Y.-S. Chen, L. Lin, J. Zhang, Y.-T. Chan, J. J. Wang, *Org. Chem.* **2018**, *83*, 4824–4830.
[28] R. Horikoshi, *Coord. Chem. Rev.* **2013**, *257*, 621–637.
[29] J. S. Mugridge, D. Fiedler, K. N. Raymond, *J. Coord. Chem.* **2010**, *63*, 2779–2789.
[30] A. Jana, S. Mandal, K. Singh, P. Das, N. Das, *Inorg. Chem.* **2019**, *58*, 2042–2053.
[31] L. Xu, Y.-X. Wang, L.-J. Chen, H. B. Yang, *Chem. Soc. Rev.* **2015**, *44*, 2148–2167.
[32] R. A. S. Vasdev, J. A. Findlay, D. R. Turner, J. D. Crowley, *Chem. Asian J.* **2021**, *16*, 39–43.
[33] J. A. Findlay, C. J. McAdam, J. J. Sutton, D. Preston, K. C. Gordon, J. D. Crowley, *Inorg. Chem.* **2018**, *57*, 3602–3614.
[34] R. Horikoshi, T. Mochida, *Eur. J. Inorg. Chem.* **2010**, 5355–5371.
[35] A. Kasprzak, P. A. Guńka, *Dalton Trans.* **2020**, *49*, 6974–6979.
[36] B. C. Patra, S. K. Das, A. Ghosh, A. R. K., P. Moitra, M. Addicoat, S. Mitra, A. Bhaumik, S. Bhattacharya, A. J. Pradhan, *J. Mater. Chem. A* **2018**, *6*, 16655–16663.
[37] D. Kaleeswaran, R. Antony, A. Sharma, A. Malani, R. Murugavel, *ChemPlusChem* **2017**, *82*, 1253–1265.
[38] R. Juarez, R. Gomez, J. L. Segura, C. Seoane, *Tetrahedron Lett.* **2005**, *46*, 8861–8864.
[39] We have also found that the volume of ethanol used for this process does not have significant influence on the reaction yield.
[40] W. A. Braunecker, K. E. Hurst, K. G. Ray, Z. R. Owczarczyk, M. B. Martinez, N. Leick, A. Keuhlen, A. Sellinger, J. C. Johnson, *Cryst. Growth Des.* **2018**, *18* (7), 4160–4166.
[41] Due to poor solubility of **Fc-2**, to prepare the samples for ^{1}H NMR analyses, **Fc-2** (*ca.* 4 mg) was sonicated for 15 minutes in 2 mL of THF-d_8 and was filtrated using a nylon membrane (pore size 0.22 μm. ^{1}H NMR spectrum revealed the presence of small-intensity peaks corresponding to the obtained product.
[42] Full spectrum is presented in Section S1, Supporting Information.
[43] See for example: J. Goubeau, E. L. Jahn, A. Kreutzberger, C. Grundmann, *J. Phys. Chem.* **1954**, *58*, 1078–1081.
[44] See for example: J. N. Willis, M. T. Ryan, F. L. Hedberg, H. Rosenberg, *Spectrochim. Acta Part A* **1968**, *24*, 1561–1572.
[45] A. J. Bard, L. R. Faulkner, **1980**. Electrochemical methods: Fundamentals and Applications; Wiley: New York.
[46] A. Kasprzak, M. K. Nisiewicz, A. M. Nowicka, *Dalton Trans.* **2021**, *50*, 2483–2492.

Manuscript received: March 23, 2021
Revised manuscript received: May 20, 2021
Accepted manuscript online: May 21, 2021